Escola de Primavera de Transição e Turbulência
Blumenau 2020

ABCM Associação Brasileira de Engenharia e Ciências Mecânicas

12th Spring School on Transition and Turbulence
September 21st-25th, 2020, Blumenau, SC, Brazil

EPTT-2020-0046
CFD INVESTIGATION OF TURBULENCE MODELING ON A GAS-LIQUID SLUG FLOW HORIZONTAL PIPE

Sarah Laysa Becker
Federal University of Santa Catarina (UFSC) – Biotério Central St., Florianópolis, SC
University of Blumenau (FURB) – São Paulo St. 3250, Blumenau, SC
sarahlaisa@gmail.com

Carla Nayara Michels dos Santos
University of Blumenau (FURB) – São Paulo St. 3250, Blumenau, SC
carlanayara.michels@gmail.com

Christine Fredel Boos
University of Blumenau (FURB) – São Paulo St. 3250, Blumenau, SC
cfboos@furb.br

Harlley Henrique Parno
University of Blumenau (FURB) – São Paulo St. 3250, Blumenau, SC
hparno@gmail.com

Vivien Rossbach
Federal University of Santa Catarina (UFSC) – Biotério Central St., Florianópolis, SC
University of Blumenau (FURB) – São Paulo St. 3250, Blumenau, SC
vivienrossbach@gmail.com

Henry França Meier
University of Blumenau (FURB) – São Paulo St. 3250, Blumenau, SC
meier@furb.br

Marcela Kotsuka da Silva
University of Blumenau (FURB) – São Paulo St. 3250, Blumenau, SC
marcelakotsuka@furb.br

Abstract. *Gas-liquid flow is characterized by the presence of specific patterns that represent interactions between the phases when they are flowing together inside a geometry. Among them, the slug pattern stands out, being characterized by intermittences of gas and liquid that can cause damage to industrial pipes and equipment. This pattern appears in vertical and horizontal pipes, and depends on operational parameters, changes in the geometry, and phase properties. Several numerical and experimental investigations have been performed to understand the hydrodynamics of slug flow. This work developed a numerical investigation of the turbulence modeling used in a horizontal pipe to capture slug flow instabilities. The simulations were performed with Reynolds-averaged Navier-Stokes (RANS), Volume of Fluid (VOF) method, and Geometric Reconstruction scheme. The simulations were compared with experimental data applying standard k-ε and k-ω Shear Stress Transport (SST) for turbulence and a case without turbulence model. Time series, power spectral density, slug frequency and translational velocity from pressure data were analyzed. All simulations, even the case with no turbulence model, captured the slug pattern, also present in the experiments, showing that slug formation was determined by instabilities of the gas-liquid flow.*

Keywords: *two-phase flow, slug pattern, computational fluid dynamics, turbulence model.*

1. INTRODUCTION

Multiphase flows are represented by the presence of two or more phases. Gas-liquid system can be found in several industrial processes. The shape of the interface between these fluids is an important characteristic called flow pattern. Pipe flows can be classified as stratified, intermittent (slug and plug), annular, bubbly, and spray (Shoham, 2006). This classification depends on pipe geometry, fluids physical properties, and flow rates. Slug is one pattern that stands out due to its intermittences that cause an unstable flow with pressure fluctuation and the possibility of erosion, vibration,

and rupture of pipelines (Abdulkadir et al., 2016). This pattern has been studied experimentally since 1950 (Baker, 1953), its mechanism of formation is related with instabilities of the flow in horizontal pipes, called Kelvin-Helmholtz instability (Kordyban and Ranov, 1970).

With the advance of technology, Computational Fluid Dynamics (CFD) simulation studies emerge as a tool to better understand the hydrodynamic of gas-liquid slug flow. Different models and conditions are applied in numerical studies to capture the behavior of slug and validate with experimental data. Hernandez-Perez et al. (2011), studied the discretization of the tridimensional domain in CFD, applying Volume of Fluid (VOF) method based on Eulerian-Eulerian approach, with High Resolution Interface Capturing Scheme (HRIC), and with the turbulence modeled by standard k-ε model. The authors created different mesh structures to compare with experiments. In conclusion, they observed that butterfly grid (O-grid) mesh achieved better results for gas-liquid flow using VOF.

Investigating slug flow, Ratkovich et al. (2013) worked with Newtonian and non-Newtonian liquids in a 2D geometry that represents a vertical duct with 19.05 mm of diameter and 3.4 m of height. VOF was also applied with the turbulence model Realizable k-ε. The numerical results showed a good agreement with experimental data comparing void fraction. In 2016, Deendarlianto et al. examined plug flow in a horizontal pipe, with 26 mm of diameter and 9.5 m of length. A CFD simulation was executed with VOF model applying k-ω SST to calculate turbulent viscosity. Volume fraction profiles, bubble size, and liquid holdup were analyzed. The authors concluded that the simulation represents the experimental data with the modeling employed.

Jaeger et al. (2018) studied gas-liquid flow in a 3D vertical geometry with 94 mm of diameter and 3 m of height. Numerical simulations used VOF model to represent the interface between the fluids. The authors analyzed different interface discretization methods and turbulence models. Comparing simulation and experiments, better results to reveal the position of the interface were obtained for the Geometric Reconstruction method. Examining turbulence, standard k-ε and k-ω SST stood out as better model options. In conclusion, the authors stated the numerical simulations represented the slug flow experiments and they can be used to characterize flow parameters.

In the same year, Pineda-Perez et al. (2018) realized a numerical study of slug flow also applying VOF, with HRIC interface scheme, and k-ω SST model. Liquid holdup, frequency, translational velocity, and velocity profile of slug pattern were investigated. Half of a cylinder, applying symmetry boundary conditions, represented the horizontal pipe geometry in simulations. The authors achieved good correlation between experiments and simulations. Extrapolating the operational conditions, they noted that the liquid made an incomplete sealing in the slug, allowing gas passage in relatively high gas velocities.

Still in 2018, Costa, Oliveira, and Barbosa investigated air-water flow in an experimental unit with 26.4 mm of diameter and approximately 5 m of length. With images of the experiments captured by a high-speed camera, the authors created an edge detection method to obtain phase distribution, slug length, frequency, and velocity. Two-phase flow simulations were also realized, applying two-fluid model combined with VOF and k-ω SST for the turbulence. The results indicated a good agreement comparing simulation and experiment images.

Santos (2019) employed CFD simulations to design a horizontal experimental unit to investigate the effect of a pipe bend with a 90° angle. VOF and Geometric Reconstruction scheme were applied with k-ω SST turbulence model. CFD helped to find an inlet geometry that does not affect slug formation. The projected experimental unit has 74 mm of diameter and 7 m of length. Finally, with the same experimental unit, Becker (2020) analyzed gas-liquid flow with different properties of the liquid by changing its viscosity and surface tension. The duct was represented by a pseudo-bidimensional geometry (2.5D). Slug frequency and translational velocity were calculated to validate the model and a good agreement was observed between physical and numerical experiments.

This study investigated turbulence approaches, analyzing their influence in horizontal two-phase slug flow. The standard k-ε and k-ω SST were employed, compared with both experimental data and a case with no turbulence model. Mathematical modelling includes VOF with the Geometric Reconstruction scheme to obtain the position of the interface between gas and liquid.

2. MATERIALS AND METHODS

Several simulations of two-phase flow were made in a geometry that represents the experimental unit's test section – a horizontal pipeline with diameter of 74 mm and 7 m of length – using air and water as working fluids. The analyzed conditions for numerical and experimental tests have superficial velocities of gas and liquid of 10 m/s and 1 m/s, respectively. The Mandhane map (Mandhane, Gregory, and Aziz, 1974) was applied to identify the flow pattern, resulting in a point in the slug flow region, as illustrated in Fig. 1.

A simplified geometry, illustrated in Fig. 2, was used to realize the simulations. The so called pseudo-bidimensional (2.5D), is an adaptation of Li et al. (2015) and Rosa (2002) geometries and was used first by Becker (2020) in gas-liquid flow. This 2.5D geometry, made by two slices connected in the middle, was applied in this work to represent a cylindrical duct, and reduce computational effort. According to Li et al. (2015), this shape is close to the 3D domain and achieves better results when compared with 2D.

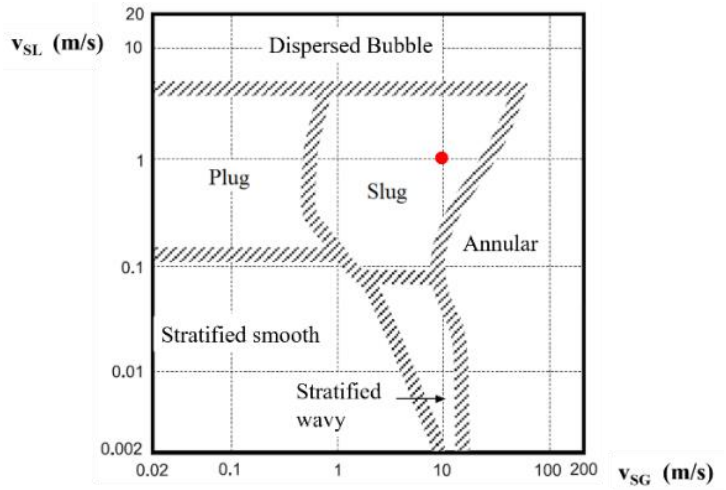

Figure 1. Mandhane map indicating the studied condition. Adapted from Mandhane, Gregory and Aziz (1974).

In this geometry, the pipe diameter of 74 mm is represented by the y-axis and the 7 m of length by the z-axis. The inlet condition was stratified, and the pipe diameter was divided in two parts, as shown in Fig. 2. The gas enters in the upper part and the liquid enters in the lower one. The outlet condition applied was static pressure equal to zero with non-slip condition at the walls. A periodic condition was employed in the sides of the geometry to allow fluid motion even in the x-axis. The periodic pairs are shown in Fig. 2. These simulations were executed in Fluent 19.1.

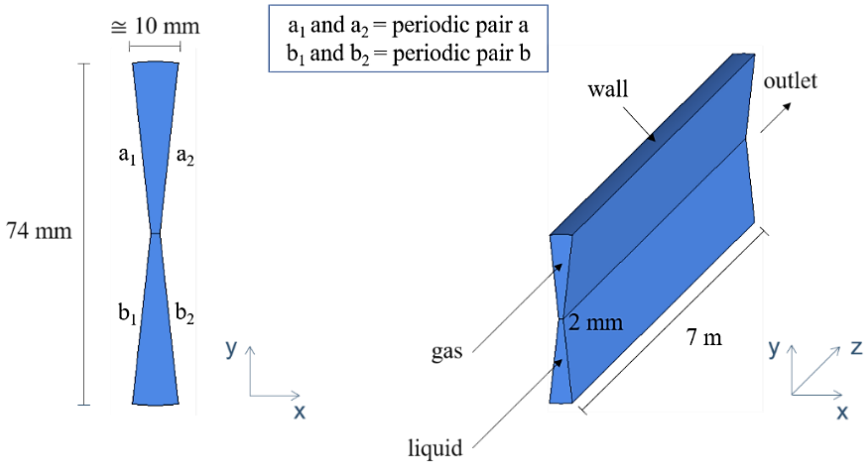

Figure 2. Pseudo-bidimensional (2.5D) geometry built for gas-liquid simulations.

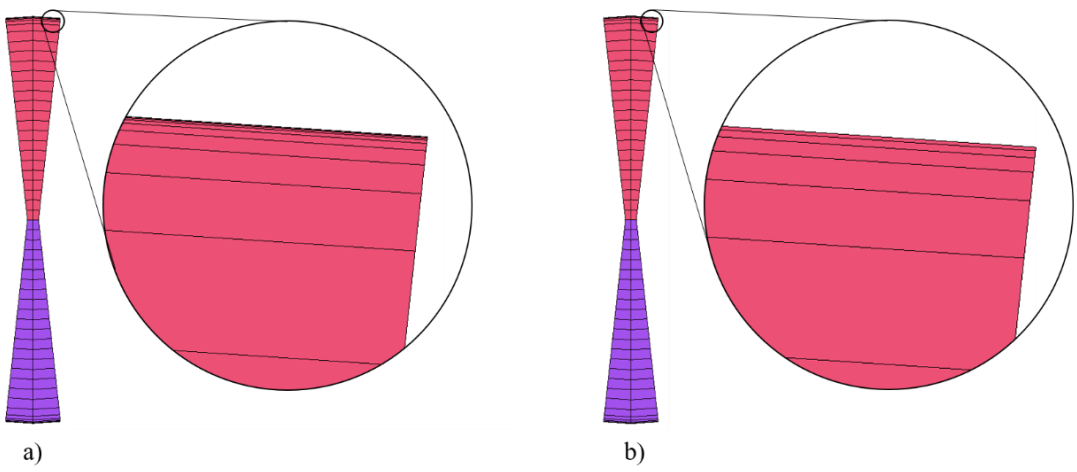

Figure 3. Numerical discretization of the 2.5D geometry for the (a) k-ω SST, and (b) k-ε turbulence model simulation.

The 2.5D geometry was discretized in two different forms to obtain suitable meshes for each turbulence model. The k-ω SST model requires an average y+ value lower than three (Menter, 1994), thus, the mesh built for it has 75600 elements, with very small elements near the wall. The k-ε model mesh has 67500 elements, resulting in an y+ lower than 100, so the wall refinement was coarse. In the case with no turbulence model (laminar), the same mesh of k-ε, with 67500 elements, was applied. Figure 3 shows the discretization of the domain in these meshes.

The simulations with different turbulence models were compared with experimental data acquired with the experimental unit developed by Santos (2019). It consists of systems for capturing liquid and gas, mixing the phases, controlling and measuring phase velocities, measuring pressure in a test section and separating the phases, showed in Fig. 4. The test section is a horizontal pipe built in transparent acrylic, seven meters long and with 74 mm internal diameter (L/D ≅ 95), allowing flow visualization from the phase mixing section to the exit to a separation drum. Experiments were run in the same conditions of the simulation, using air and water as fluids. Data acquisition was carried out with three pressure transducers installed on top of the test section tube at 6.8, 5.8 and 4.8 m from the mixing section, at a 1 kHz sampling rate using a USB-6211 National Instruments® board and virtual instrument developed using LabVIEW® software.

Data acquisition of the experiments started when the superficial velocities were stable and two-phase flow was fully developed. Three repetitions were made to ensure repeatability of the phenomenon. A blue food dye was added to the water for better visualization of the flow. This addition did not change any property of the fluid. The simulations started with air and water entering the geometry in a stratified form. Just as executed in the physical experiments data was analyzed only after the phases filled the pipe and the flow was developed.

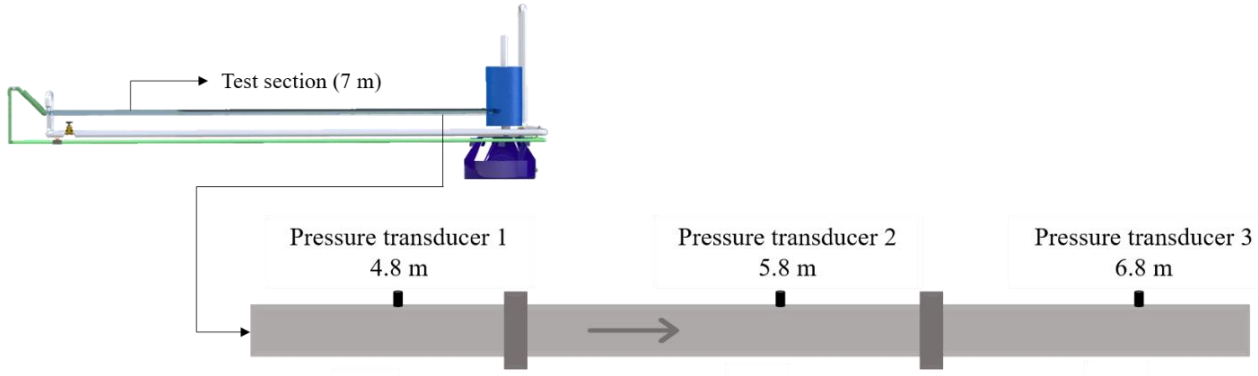

Figure 4. Experimental test section with the arrangement of the pressure transducers.

The pressure signals from both the experiments and simulations were used to calculate slug frequency and translational velocity applying the method described in Becker (2020). In brief, slug frequency is a measure of slugs, represented by pressure peaks, passing through a point in the pipe. The translational velocity is the velocity of the liquid slug front, which was estimated analyzing pressure peaks that represent the passage of the same slug by two transducers related with the distance between them. This value is an average of all slugs computed by the method.

Translational velocity results were compared with a correlation presented by Nicholson, Aziz, and Gregory (1978) applying drift velocity defined by Benjamin (1968), as described in Eq. (1):

$$v_{ts} = 1.2v_M + 0.54\sqrt{gD} \tag{1}$$

where v_M is the mixture velocity represented by the sum of superficial velocities of gas and liquid, g is gravitational acceleration, and D is the pipe diameter.

Time series and normalized amplitude Power Spectral Density (PSD) were also used to compare experiments and simulations, employing a percentage error to quantify possible disparities. This error was calculated by the module of the difference between expected and obtained values, divided by the expected value.

3. MATHEMATICAL MODEL

The mathematical model required for the simulations includes the conservation of mass and momentum, applying Reynolds average and assuming Boussinesq hypothesis to model turbulence (Moukalled, Mangani, and Darwish, 2016), as described by Eq. (2) and (3):

$$\frac{\partial \rho}{\partial t} + \nabla.(\rho \boldsymbol{v}) = 0 \tag{2}$$

$$\frac{\partial}{\partial t}(\rho \boldsymbol{v}) + \nabla.(\rho \boldsymbol{v}\boldsymbol{v}) = -\nabla p + \nabla.\mu_{eff}(\nabla \boldsymbol{v} + \nabla \boldsymbol{v}^T) + \rho \boldsymbol{g} \quad (3)$$

in which t is time, ρ is density, $\boldsymbol{v}$ is the average velocity vector, p is the average static pressure, and μ_{eff} is the effective viscosity, that is determined by the sum of molecular viscosity (μ) and turbulent viscosity (μ^T).

The Volume of Fluid (VOF), proposed by Hirt and Nichols (1981), was employed to predict the interface between two phases. This method was used by many authors for gas-liquid flow (Ratkovich *et al*., 2013; Deendarlianto *et al*., 2016; Pineda-Perez *et al*., 2018; Jaeger *et al*., 2018; Santos, 2019; Becker, 2020). VOF introduces a function in the governing equations that describes volume fraction of the phase i present in a mesh cell (α_i), as demonstrated by Eq. (4). Therefore, when there is no fluid i in a cell, the value of α_i is zero. If the cell is full of fluid i, α_i is equal to one. And if there is an interface in a cell, the value of α_i is between 0 and 1, representing the volume fraction of the fluid i.

$$\frac{\partial}{\partial t}(\alpha_i \rho_i) + \nabla.(\alpha_i \rho_i \boldsymbol{v}) = 0 \quad (4)$$

The scheme applied to represent the position of the interface between fluids, solving Eq. (4), was the Geometric Reconstruction. This method was deemed appropriate to represent gas-liquid flow by Venturi (2015) and Jaeger *et al.* (2018). Presented by Youngs (1982), it considers a well-defined interface and gives its position considering the interest cell and neighboring cells volume fractions. In a 2D cell, for example, the interface is represented by a straight line.

Based on Jaeger *et al*. (2018), Standard k-ε and k-ω SST turbulence models were compared for the gas-liquid horizontal flow. These two models were analyzed, to represent the effect of the eddies and calculate turbulent viscosity (μ^T). One numerical case without a turbulence model was also analyzed, applying laminar condition in Fluent 19.1. Although the superficial Reynolds number of the phases correspond to turbulent flow (73645.86 for the water and 50642.46 for the air), this condition was applied with the aim of calculate turbulence by the conservation equations with the mesh refinement. The mesh applied was coarse and possibly not enough to calculate small eddies, but slug is a big structure and depends on flow instabilities.

In the Standard k-ε model (Jones and Launder, 1972), turbulent viscosity was modeled by the following equation:

$$\mu^T = C_\mu \frac{k^2}{\varepsilon} \quad (5)$$

where k represents turbulent kinetic energy, ε its dissipation rate, and C_μ is an empirical constant with value 0.09, suggested by Jones and Launder (1972). Values of k and ε where obtained by additional transport equations:

$$\frac{\partial}{\partial t}(\rho k) + \nabla.\left[\rho \boldsymbol{v} k - \left(\mu + \frac{\mu^T}{\sigma_k}\right)\nabla k\right] = P^k - \rho\varepsilon \quad (6)$$

$$\frac{\partial}{\partial t}(\rho \varepsilon) + \nabla.\left[\rho \boldsymbol{v} \varepsilon - \left(\mu + \frac{\mu^T}{\sigma_\varepsilon}\right)\nabla \varepsilon\right] = C_1 \frac{\varepsilon}{k} P^k - C_2 \rho \frac{\varepsilon^2}{k} \quad (7)$$

in which the constants values were: σ_k = 1.0, σ_ε = 1.3, C_1 = 1.44, and C_2 = 1.92, and P^k is calculated by Eq. (8):

$$P^k = \mu^T(\nabla \boldsymbol{v} + (\nabla \boldsymbol{v})^T) : \nabla \boldsymbol{v} \quad (8)$$

The k-ω Shear Stress Transport (SST) model blends k-ε and k-ω models, using the first one in the core of the domain and the second one near the walls (Menter, 1994). Turbulent viscosity was obtained by Eq. (9).

$$\mu^T = \frac{a_1 k}{Max(a_1 \omega, SF_2)} \quad (9)$$

considering a_1 as a model constant, and S the invariant measure of the strain rate. In order to calculate k and ω, additional transport equations need to be solved:

$$\frac{\partial}{\partial t}(\rho k) + \nabla.\left[\rho \boldsymbol{v} k - \left(\mu + \frac{\mu^T}{\sigma_k}\right)\nabla k\right] = \tilde{P}_k - \beta^* \rho k \omega \quad (10)$$

$$\frac{\partial}{\partial t}(\rho \omega) + \nabla.\left[\rho \boldsymbol{v} \omega - \left(\mu + \frac{\mu^T}{\sigma_\omega}\right)\nabla \omega\right] = \beta_1 \frac{\omega}{k} P_k - \beta_2 \rho \omega^2 + 2(1 - F_1)\sigma_{\omega 2} \frac{\rho}{\omega} \nabla k.\nabla \omega \quad (11)$$

F_1 and F_2 are blending functions:

$$F_1 = \tanh\left(\left\{Min\left[Max\left(\frac{\sqrt{k}}{\beta^*\omega(d_\perp)}, \frac{500\nu}{(d_\perp)^2\omega}\right), \frac{4\rho\sigma_{\omega 2}k}{CD_{k\omega}(d_\perp)^2}\right]\right\}^4\right) \quad (12)$$

$$F_2 = \tanh\left(Max\left(2\frac{\sqrt{k}}{\beta^*\omega(d_\perp)}, \frac{500\nu}{(d_\perp)^2\omega}\right)^2\right) \quad (13)$$

with $CD_{k\omega} = Max(2\rho\sigma_{\omega 2}\nabla k.\nabla\omega/\omega, 10^{-10})$, $d_\perp$ represents the distance to the nearest wall, the constants β^* = 0.09, $\sigma_{\omega 2}$ = 0.856, and the others (σ_k, σ_ω, β_1, β_2) are obtained by a blend of constants from k-ε and k-ω models.

4. RESULTS AND DISCUSSION

Flow pattern was identified visually in the experiments by images of the last meters of the test section, as illustrated in Fig. 5, while contours of volume fraction were used for pattern identification in the simulations, as shown in Fig. 6, 7, and 8. Three cases with different turbulence approaches and the experiment presented slug flow for superficial velocities of gas and liquid of 10 m/s and 1 m/s, respectively. These results agree with the prediction of Mandhane map.

In the experiments, the slug formation happens even in the inlet of gas and liquid (0 m). The slug structure is aerated, presenting a type of foam formed by the flow in the slug front. A thin liquid film was observed in the upper part of the pipe, near the wall.

Contours of water volume fraction were built to analyze the slug flow in the simulations. Those were made in an aleatory flow time, just to show a slug passing through the pipe, as illustrated by Fig. 6, 7 and 8. The contours are also used to determine the time necessary to develop slug flow and its formation, that occurs after a certain pipe length. The slugs observed in the k-ε case (Fig. 6) were more aerated, at times, over its passage through the pipe, the liquid did not close the entire cross section of the pipe. In this case, slug flow developed in 3.2 s and its formation happened after 2.5 m of pipe length.

For k-ω SST model simulation, illustrated in Fig. 7, the slugs are also aerated, the development occurred in 8.6 s with formation only after 3.5 m. In the case simulated with no turbulence model (Fig. 8), the liquid slug closes the cross section of the pipe and a liquid film was observed in the upper part, near the walls, as noted in the experiment. The flow development occurred in 4.5 s and the slug structures formed after 1.5 m of pipe length. These differences in the point of slug formation between simulations and experiments can be attributed to the inlet and the simplifications made in the simulation geometry.

The appearance of slug structures in the case with no turbulence model with a coarse mesh (Fig. 8) demonstrates that its formation was strongly linked to instabilities created in the flow, that are responsible for the development of a wave that grows and closes the pipe cross section. A slug was not formed just by turbulence, these instabilities have a large influence under its development.

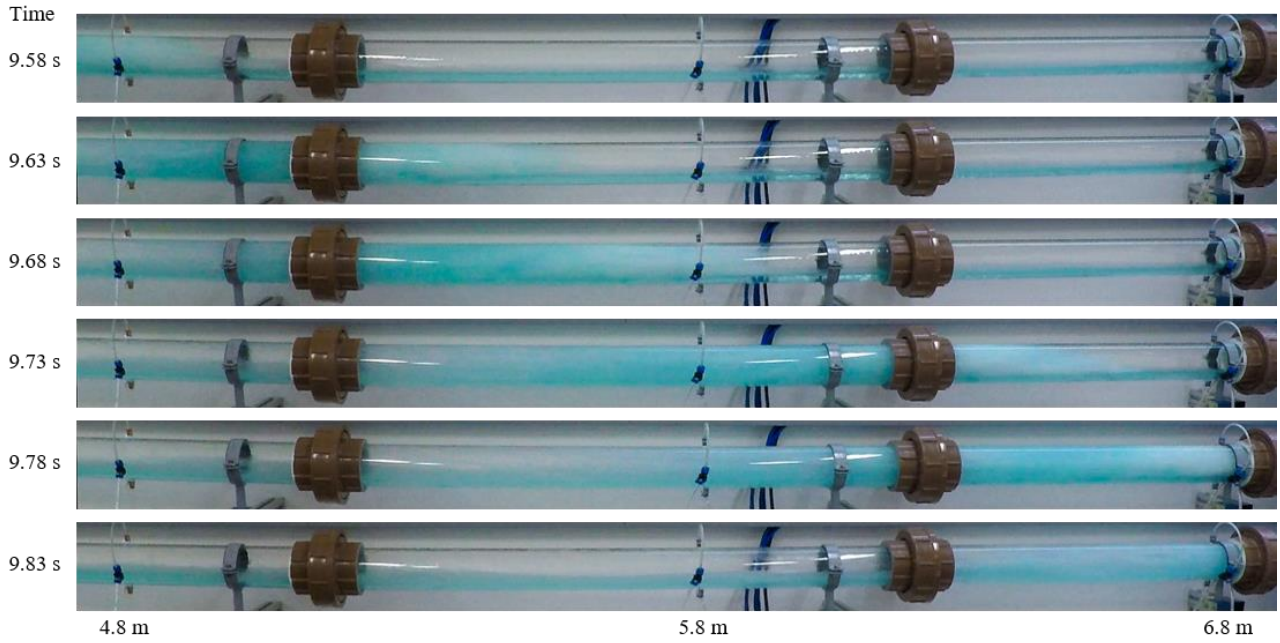

Figure 5. Passage of a slug in the test section with superficial velocities of gas and liquid of 10 m/s and 1 m/s.

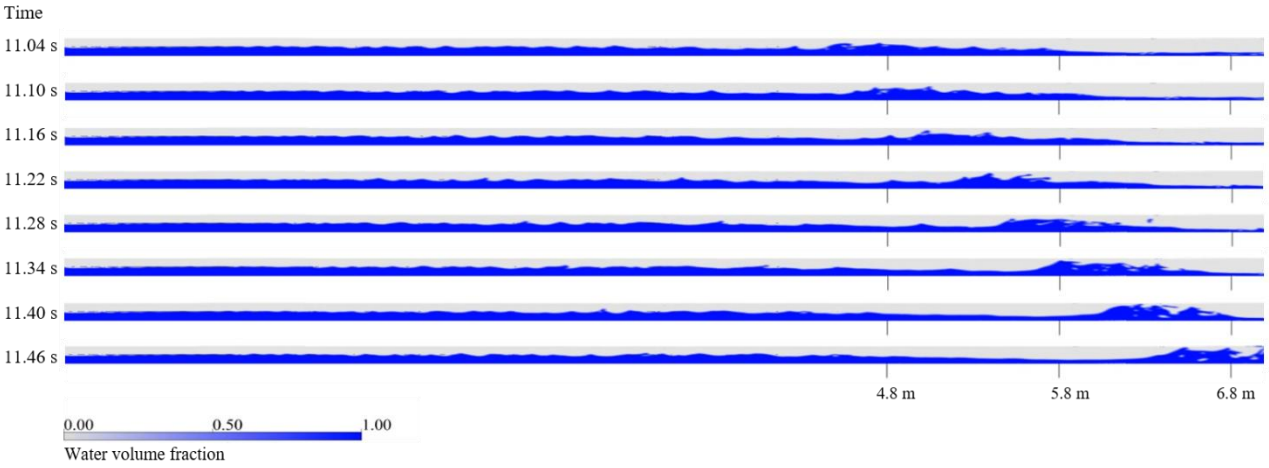

Figure 6. Contours of water volume fraction for the case with k-ε turbulence model.

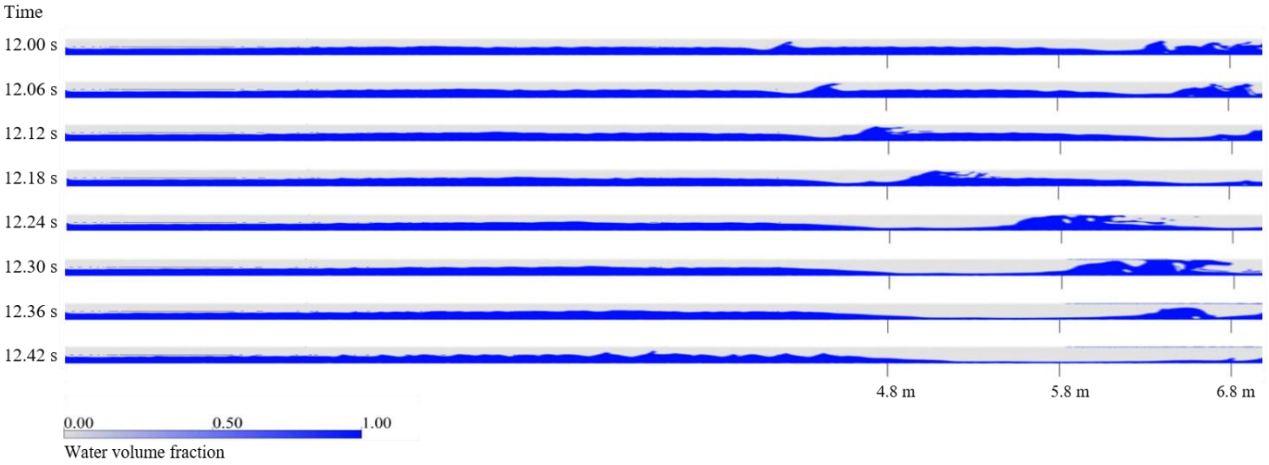

Figure 7. Contours of water volume fraction for the case with k-ω SST turbulence model.

Figure 8. Contours of water volume fraction for the case with no turbulence model.

Pressure signal was investigated in both physical and numerical experiments, by analyzing the peaks that represent slug pattern. The first repetition of the experiment is compared with all simulations in Fig. 9, which shows the pressure signal measured at 5.8 m from the mixing section, in the upper part of the pipe. This point was chosen because a preliminary analysis showed that at this point the flow is fully developed – some slugs are formed only after 4.8 m – and the possibility of flow interference caused by the outlet's geometry is minimal. The analyzed pressure signals correspond to 10 s after an initial time interval of 8.6 s necessary to stabilize the flow in all the simulation cases.

The peaks amplitude changed between simulations and experiments. The latter had small pressure peaks (Fig. 9 – a) and the case with no turbulence model had the highest ones (Fig. 9 – d). The case with k-ε (Fig. 9 – b) presented the smaller peaks when compared with the other simulations, with some of them being close to the ones present in the experiment's signal. The pressure signal of k-ω SST case (Fig. 9 – c) was similar to the one of the simulation with no turbulence model, but still has slug peaks with smaller amplitude like the physical experiment.

The fact that the absence of a turbulence model generated higher peaks can be attributed to the visual observation that slugs in this case are well-shaped and fill the pipe's cross section with a higher amount of liquid, as noted in the contours of Fig. 8. The time series of this case showed that slugs happen in some seconds, then they stop, the flow becomes stratified, and then started again. The contours also showed that when a slug passes, the liquid level in the pipe reduces, so this pause corresponds to a moment when the liquid returns to its normal level to form waves that become new slug structures. The cases with turbulence model and the experiment also present seconds of stratified flow in between slugs, but not so long or so frequent. This might have occurred due to the higher quantity of liquid existent in the slugs of the case with no turbulence model.

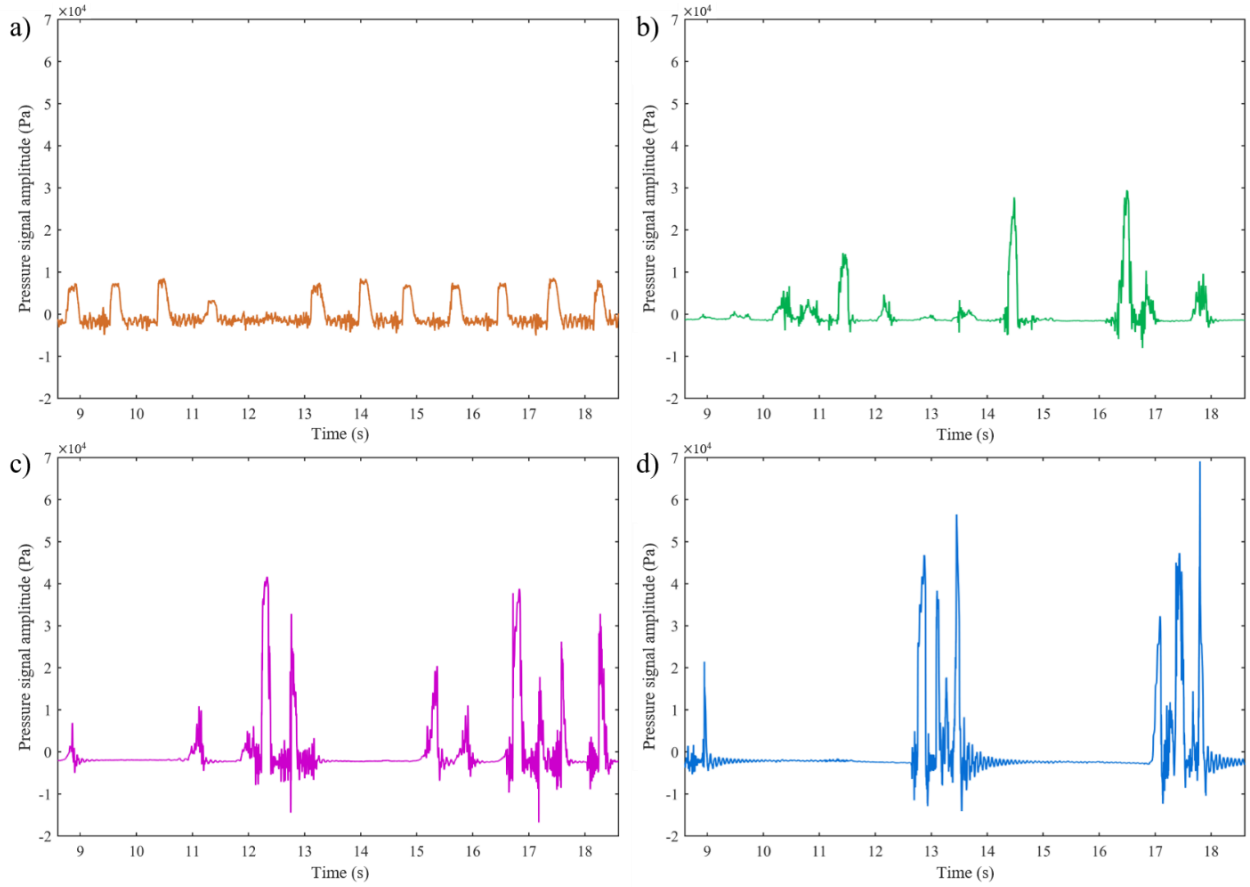

Figure 9. Pressure signals of the a) physical experiment's first repetition, b) simulation with k-ε model, c) simulation with k-ω SST model, and d) simulation with no turbulence model.

Power spectral density (PSD) of the pressure signals was also analyzed. Some authors, based on their experiments, linked the slug flow with PSD prominent frequencies around 1 Hz and related this number to the slug frequency (Abdulkadir *et al*., 2016; Jaeger *et al*., 2018; Santos, 2019; Becker, 2020). A prominence around 1.2 Hz was observed in the experiment, as shown in Fig. 10 – a. The k-ε case (Fig. 10 – b) had a prominent frequency close to the experiment, of 1.0 Hz, while the cases with no turbulence model (Fig. 10 – d) and k-ω SST (Fig. 10 – c) had more distant prominences, of 0.2 Hz and 2.0 Hz, respectively.

Slug frequency was calculated counting slug representative pressure peaks that passed through the 5.8 m measure point. A comparison of physical and numerical experiments' slug frequencies and PSD prominent frequency is shown in Tab. 1. The experimental value presented is the average and standard deviation of the three repetitions. All slug frequencies were obtained using the same method and the ten seconds of pressure signal.

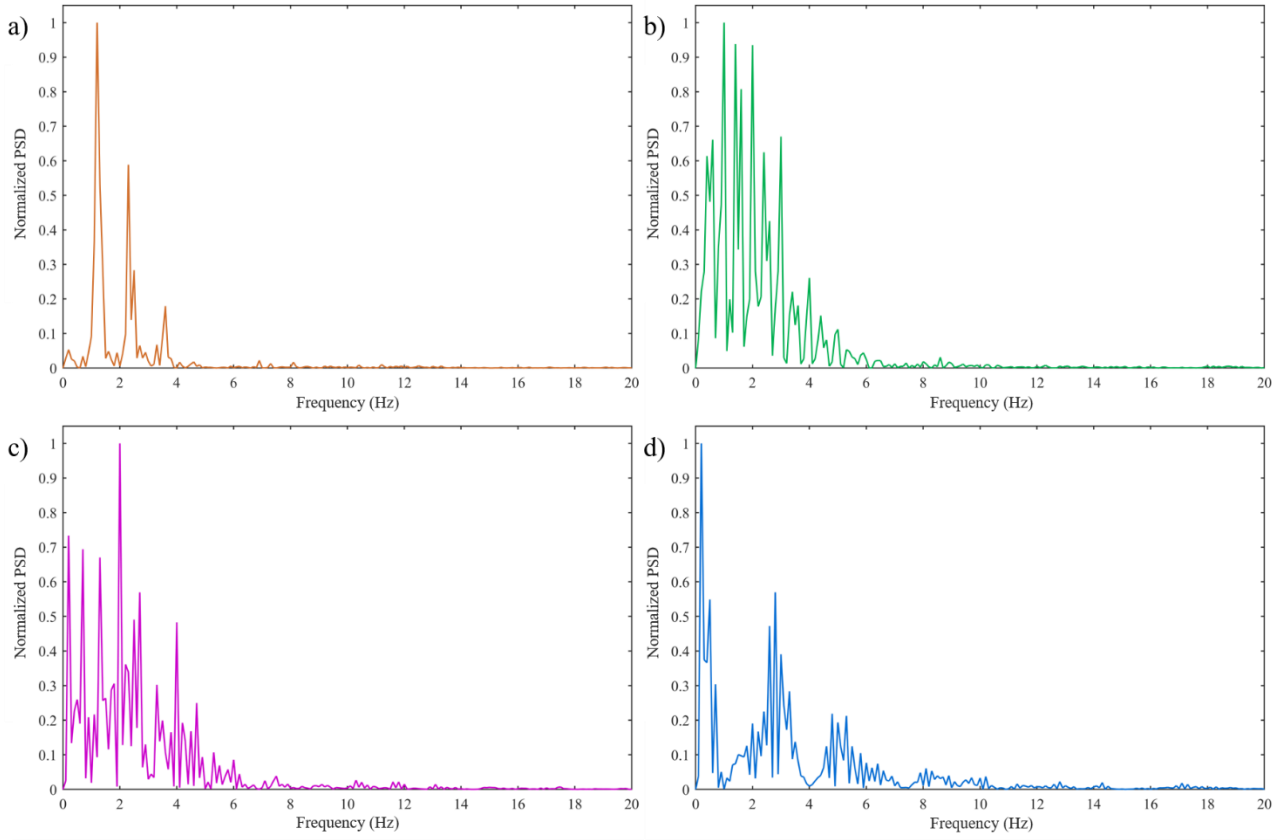

Figure 10. PSD of the pressure signal of the a) experiment first repetition, b) simulation with k-ε model, c) simulation with k-ω SST model, and d) simulation with no turbulence model.

The PSD prominence and slug frequency had similar values between experimental and k-ε model case. However, a large difference was observed in the cases with k-ω SST and no turbulence model, an error of 66.70% and 81.82%, respectively. In these cases, the PSD frequency did not represent the number of slugs flowing through the measure point. This can be confirmed by observing the contours of volume fraction and counting the slugs that pass through the pipe. These slugs correspond to the peaks observed in the corresponding pressure time series. Analyzing the values obtained by counting peaks, it was found that the simulations are close to the experiment. The case with no turbulence model achieved a better result, with an error of 2.94%. When the slug frequency was compared to the PSD prominence, the k-ε turbulence model has the best performance, with an error of 16.65%.

Table 1. Results of slug and PSD prominence frequency in experiments and simulations.

Data	Slug frequency (Hz)	PSD prominence (Hz)
Experiments	1.1333 ± 0.0577[(1)]	1.2002 ± 0.0000[(1)]
k-ε model	0.9000	1.0002
k-ω SST model	1.2000	2.0004
No turbulence model	1.1000	0.2000

[(1)]Average ± standard deviation of the three experimental repetitions.

The slug translational velocities calculated with 10 s of developed flow are presented in Tab. 2. The data from the experiments' pressure transducers and simulations' monitoring points located at 5.8 and 6.8 m of pipe length are applied to calculate this slug flow characteristic. The velocity obtained by Nicholson, Aziz, and Gregory (1978) and Benjamin (1968) correlation was also presented. Once again, the experimental value corresponds to the average and standard deviation of the three repetitions.

It was found that experiments' average and correlation values presented a difference of 23.21%. The turbulence model did not influence the translational velocity, however when comparing with the experimental data all the numerical tests showed higher values: the k-ε case presented an error of 47.01%, the k-ω SST case had a 44.40% difference, and the case with no turbulence model had the smallest error, of 43.49%.

Table 2. Results of slug translational velocity in experiments and simulations.

Data	Slug translational velocity (m/s)
Correlation	13.6601
Experiment	$10.4890 \pm 0.3592^{(1)}$
k-ε model	15.4208
k-ω SST model	15.1470
No turbulence model	15.0512

(1)Average ± standard deviation of the three experimental repetitions.

5. CONCLUSIONS

Slug flow experimental data were compared with three simulations, each using different turbulence approaches. A horizontal geometry was analyzed in the condition of gas and liquid superficial velocities of 10 m/s and 1 m/s. Pressure signals were used to calculate slug frequency and translational velocity, as well as allow a PSD prominence and time series' morphology analysis.

Volume fraction contours were compared with images of the flow in the test section of the experimental unit. All numerical cases and experiments presented the slug pattern, even the case with no turbulence model, indicating that slug formation is determined by instabilities of the flow. Both cases with turbulence model showed a more aerated slug, similar to the experiments. Although the slug in the case with no turbulence model is more liquid, with a complete filling of the cross section of the pipe, it was noted a thin liquid film near the wall that was also observed in the experiments.

The time series and PSD were analyzed to understand the effect of slug pattern in the pressure values measured in the upper part of the pipe. The k-ε and k-ω SST cases had a smaller signal amplitude than the case with no turbulence model, with k-ε being closer to the experimental data. In the PSD comparison, just the case with k-ε turbulence model showed prominent frequencies around 1 Hz, which also appeared in the experiments and, according to literature, is related to the slug flow pattern.

Slug frequency was compared between experiments and simulations in two methods: the first calculated by counting pressure peaks and the second by the PSD. These two methods obtained similar values for the experiment and the case with k-ε turbulence model. In the other simulations the PSD prominence did not correspond to the slug frequency. Analyzing the slug frequency calculated by corresponding pressure peaks, the case with no turbulence model stood out with a value near to the experiments' average (2.94% difference). Finally, analyzing slug translational velocity, the values obtained in simulations were different from the experiments' average, with errors between 43.49% and 47.01%.

Based on the comparison results of this study, the k-ε model was the best one since it reached good results in the majority of comparisons. However, a definitive conclusion about the best turbulence model for horizontal flow needs further analysis such as the quantification of the numerical solution's uncertainty related to the mesh refinement.

6. ACKNOWLEDGEMENTS

The authors are grateful for the financial support of PETROBRAS (research project grant number 5850.0103010.16.9) and Coordenação de Aperfeiçoamento de Pessoal de Nível Superior (CAPES).

7. REFERENCES

Abdulkadir, M., Hernandez-Perez, V., Lowndes I. S., Azzopardi, B. J., and Sam-Mbomah, E., 2016. "Experimental study of the hydrodynamic behavior of slug flow in a horizontal pipe". *Chemical Engineering Science*, Vol. 156, p. 147-161.

Baker, O., 1953. "Design of Pipelines for Simultaneous Flow of Oil and Gas". *Oil & Gas Journal*, p. 185-201.

Becker, S. L., 2020. *Estudo dos Efeitos das Propriedades Físicas do Líquido Sobre a Dinâmica do Escoamento Bifásico em Duto Horizontal.* Master's dissertation, University of Blumenau, Blumenau.

Benjamin, T. B., 1968. "Gravity currents and related phenomena". *Journal of Fluid Mechanics*, Vol. 31, p. 209-248.

Deendarlianto, A., Andrianto, M., Widyaparaga, A., Dinaryanto, O., Jaelani, J., and Indarto, 2016. "CFD Studies on the Gas-liquid plug two-phase flow in a horizontal pipe". *Journal of Petroleum Science and Engineering*, Vol. 147, p. 779-787.

Hernandez-Perez, V., Abdulkadir, M., Azzopardi, B. J., 2011. "Grid Generation Issues in the CFD Modelling of Two-Phase Flow in a Pipe". *The Journal of Computational Multiphase Flows*, Vol. 3, p. 13-26.

Hirt, C. W., and Nichols, B. D., 1981. "Volume of fluid (VOF) method for the dynamics of free boundaries". *Journal of Computational Physics*, Vol. 39, p. 201-225.

Jaeger, J., Santos, C. M., Rosa, L. M., Meier, H. F., and Noriler, D., 2018. "Experimental and numerical evaluation of

slugs in vertical air-water flow". *International Journal of Multiphase Flow*, Vol. 101, p. 152-166.

Jones, W. P., and Launder, B. E., 1972. "The prediction of laminarization with a two-equation model of turbulence". *International Journal of Heat and Mass Transfer*, Vol. 15, p. 301-314.

Kordyban, E., and Ranov, T., 1970. "Mechanism of Slug Formation in Horizontal Two-Phase Flow". Journal of Basic Engineering, Vol. 92, p. 857-864.

Li, T., Benyahia, S., Dietiker, J. F., Musser, J., and Sun, X., 2015. "A 2.5D computational method to simulate cylindrical fluidized beds". *Chemical Engineering Science*, Vol. 123, p. 236-246.

Mandhane, J. M., Gregory, G. A., and Aziz, K., 1974. "A flow pattern map for gas-liquid flow in horizontal pipes". *International Journal of Multiphase Flow*, Vol. 1, p. 537-553.

Menter, F. R., 1994. "Two-equation eddy-viscosity turbulence models for engineering applications". *American Institute of Aeronautics and Astronautics (AIAA) Journal*, Vol. 32, p. 1598-1605.

Moukalled, F., Mangani, L., Darwish, M., 2016. *The Finite Volume Method in Computational Fluid Dynamics: An Advanced Introduction with OpenFOAM and Matlab*. Springer, Switzerland.

Nicholson, M. K., Aziz, K., Gregory, G. A., 1978. "Intermittent two-phase flow in horizontal pipes: Predictive models". *The Canadian Journal of Chemical Engineering*, Vol. 56, p. 653-663.

Pineda-Perez, H., Kim, T., Pereyra, E., and Ratkovich, N., 2018. "CFD modeling of air and water highly viscous liquid two-phase slug flow in horizontal pipes". *Chemical Engineering Research and Design*, Vol. 136, p. 638-653.

Ratkovich, N., Majumder, S. K., and Bentzen, T. R., 2013. "Empirical correlations and CFD simulations of vertical two-phase gas-liquid (Newtonian and non-Newtonian) slug flow compared against experimental data of void fraction". *Chemical Engineering Research and Design*, Vol. 91, p. 988-998.

Rosa, L. M., 2002. *Simulação de Reações Químicas e Consumo de Calor em Risers.* Master's dissertation, University of Campinas, Campinas.

Santos, C. N. M., 2019. *Estudo Experimental e Numérico do Efeito do Duto de Saída Sobre a Dinâmica do Escoamento Bifásico em Duto Horizontal*. Master's dissertation, University of Blumenau, Blumenau.

Shoham, O., 2006. *Mechanistic Modeling of Gas-liquid Two-phase Flow in Pipes*. Society of Petroleum Engineers, Tulsa.

Venturi, D. N., 2015. *Análise Numérica e Experimental da Fluidodinâmica em Feixe de Tubos com Abordagem de Volume de Fluido (VOF).* Master's dissertation, University of Blumenau, Blumenau.

Youngs, D. L., 1982. "Time-dependent multi-material flow with large fluid distortion". *Numerical Methods for Fluid Dynamics*, p. 273-285.

8. RESPONSIBILITY NOTICE

The authors are the only responsible for the printed material included in this paper.